

# A 5/4 commensurability of KIC 5773205, the smallest eclipsing red dwarf detected by the Kepler mission

Valeri V. Makarov

valeri.makarov@navy.mil

*US Naval Observatory, 3450 Massachusetts Ave NW, Washington DC 20392-5420, USA*

Alexey Goldin

alexey.goldin@gmail.com

*Teza Technology, 150 N Michigan Ave, Chicago IL 60601, USA*

Accepted . Received ; in original form

## ABSTRACT

KIC 5773205 is the least luminous eclipsing M dwarf found in the Villanova catalog of eclipsing binaries detected by the *Kepler* mission. We processed and analyzed the three available quarters of mission data for this star and discovered a persistent periodic variation of the light curve with a period, which is in exact 4:5 commensurability to the orbital period. Three routes of interpretation are considered: 1) non-radial pulsations excited by the tidal interaction at a specific eigenfrequency; 2) a high-order spin-orbit resonance caused by the tides; 3) an ellipsoidal deformation caused by an outer orbiting companion in a mean motion resonance. All three explanations meet considerable difficulties, but the available facts seem to favor the tidally driven pulsation scenario. The star may represent a new type of heartbeat binary with tidally excited pulsations that are close to the orbital motion in frequency.

## 1. Introduction

The third version of the eclipsing star catalog detected by the Kepler mission includes 2787 systems (Kirk et al. 2016). The primaries in these systems represent various luminosity classes and evolutionary states of Galactic stellar population, including the main sequence, giants and subgiants, and hot subdwarfs (sdO and sdB). However, the small stars that are found at the bottom of the main sequence and degenerate stars are rare in this catalog. There are only two binaries among those present in the Gaia DR2 catalog with absolute  $G$ -band magnitudes ( $M_G$ ) fainter than 10. One of them, KIC 10544976, is a known WD+M binary (Ritter & Kolb 2003; Parsons et al. 2015) with an orbital period of 0.3504691 d (Slawson et al.

2011) and interesting out-of-eclipse ellipsoidal variations (Lurie et al. 2017). The other, KIC 5773205, which is the subjects of this paper, is less well known. Its eclipse period in Kirk et al. (2016) is  $0.2668707(17)$  d<sup>1</sup>, which is closer to the short end of the distribution. No secondary eclipses are present, hinting at a considerable eccentricity. The eclipse time variation data from Conroy et al. (2014) do not show any discernible signal.

Although M dwarfs are very common in the Galaxy and in the Solar neighborhood in particular (Henry et al. 2006), there are not many known eclipsing binaries with late M dwarfs as primaries. This is explained by their relatively small size, faintness, and the limited range of the mass function for the companion. KIC 5773205 matches the Gaia DR2 source 2103827298302304128 with the full complement of astrometric and photometric measures. Its observed parallax  $\varpi = 2.83(21)$  mas, broadband  $G$  magnitude 18.7750(26), and the color  $BP - RP = 3.19(17)$  mag, identifies this star as an M4.5V dwarf with an effective temperature of  $\sim 3100$  K according to E. Mamajek’s stellar data, but the estimated absolute luminosity  $M_G \simeq 11.04$  mag suggests a slightly larger dwarf of the M3.5V type. Thus, the absolute magnitude seems slightly too luminous for the observed color. This excess brightness may be attributed to the presence of another dwarf in the binary system. Generally, the star appears at first sight to be a nondescript field dwarf at 352 pc from the Sun, lacking distinguishing features such as enhanced X-ray or ultraviolet radiation.

The long-cadence light curve is available for three quarters of the *Kepler* mission: Q14, Q15, Q16. We use the raw Simple Aperture Photometry (SAP) Kepler light curves rather than the Pre-search Data Conditioning (PDC) fluxes derived by the data processing pipeline (Christiansen et al. 2012). To remove the slow variations of flux in the raw data, we employ our own Principal Component Analysis (PCA) pre-whitening and filtering procedure described in more detail in Makarov & Goldin (2016b, 2017). We always use 4 principal components for both astrometric and photometric data divided into quarter-year segments ( $\sim 90$  days). The resulting cleaned light curves and astrometric trajectories are further analyzed in this paper.

## 2. Variability-induced motion (VIM) test

Three kinds of variability are clearly present in the light curves of KIC 5773205: 1) periodic eclipses caused by the binary companion; 2) small and moderate flares; 3) a quasi-periodic signal. All these variations are also visible in the measured photocenter coordinates. The synchronous and correlated behavior of the measurements is a natural consequence of the first-moment estimation technique coupled with a limited sample area. Photometry and astrometry with Kepler are interdependent because a small motion of the digital aperture (due to the differential aberration or a pointing jitter) changes the amount of collected light, while any

---

<sup>1</sup>Throughout this paper, numbers in round brackets stand for standard errors of values in the last significant digits, i.e., 1.549(65) is equivalent to  $1.549 \pm 0.065$

intrinsic variation of the stellar flux shifts the measured photocenter. The latter is exacerbated by the low angular resolution and rather large digital apertures, which include parts of chance neighbors’ images. The fraction of blended light also depends on the orientation of the aperture on the sky for the same configuration of stars. Therefore, the observed photocenter location changes between the quarters by great amounts compared to the expected photon noise level. The correlated motion of photocenter centroids and variation of flux provides an easy way of testing the origin of this variability in the simplest and most common case when one of the neighbors dominates the blended flux. If the intended target (close to the center of the aperture) is variable and becomes brighter, the photocenter moves toward it along the line connecting it with the dominant neighbor. If it is the neighbor that becomes brighter, the photocenter moves in the opposite direction. Generally, the centroid moves toward the brightening source, but the picture becomes complicated when a few competing blends are present or only some part of the blended image is covered by the aperture.

Our comprehensive analysis of VIMs in the main mission data (Makarov & Goldin 2016a) detected two instances for KIC 5773205 in quarters Q14 and Q15 with position angles (counted counterclockwise as seen on the sky, north through east) of  $280^\circ$  and  $267^\circ$ . This analysis for KIC 5773205 is further complicated by the fact that the “optimal” digital aperture, where the flux was determined, includes only a single pixel, which was apparently meant to lower the impact of brighter neighbors. We implemented a much improved reprocessing of VIM effects in the long-cadence data consistently using our PCA cleaning method and discarding all saturated objects, to be published elsewhere. This new reprocessing resulted in a confident detection for all three available quarters:  $280^\circ$  in Q14,  $267^\circ$  in Q15, and  $271^\circ$  in Q16. We note a good consistency with the previous result and persistent, even though slightly scattered, direction of the correlated astrometric wobble. The Gaia DR2 catalog (Brown & Gaia Collaboration 2018), as well as the Pan-STARRS DR2 catalog and online stacked charts (Chambers et al. 2016) reveal the presence of two slightly brighter optical (unrelated) companions at separations  $8''.893$ ,  $12''.919$  and position angles  $83.5^\circ$ ,  $156.0^\circ$  from our object of interest. A few much fainter objects are also present within the Kepler digital aperture, but they hardly matter. It appears that the closer optical companion, which is brighter than the target by 0.619 mag in  $G$ , is the main source of the observed VIM, with a smaller contribution from the more distant blue neighbor. The important fact is that these perturbing neighbors are situated in the opposite direction to the observed VIM. This confirms that the photometric variability detected by *Kepler* belongs to the intended target.

### 3. Photometric variability

The Villanova Catalog of Eclipsing Binaries lists KIC 5773205 with a period  $P_o = 0.2668707(17)$  d and an eclipse depth of 0.0478 (Kirk et al. 2016). The eclipse is clearly visible if we fold the light curve with this period, see Fig. 1, left. There is a scatter of data points well above the folded light curve, which is caused by short-term flares of moderate magnitude. There is

no obvious periodicity or order in the occurrence of flares. There is a previously unnoticed third type of variability, which we investigate in this paper. It causes the apparently uniform dispersion of flux measurements within  $\sim 10$  electrons per second in the folded light curve.

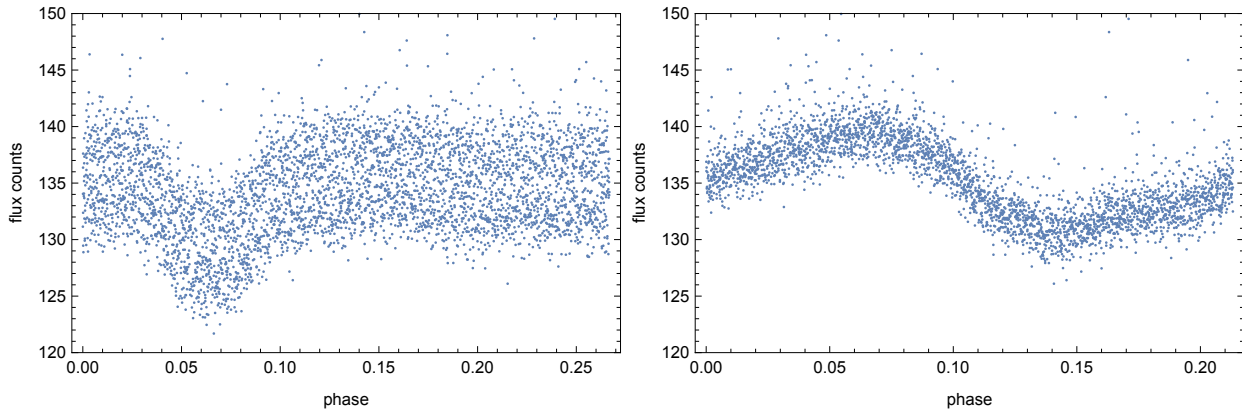


Fig. 1.— Folded light curves of KIC 5773205 for quarter Q14. Left: The complete cleaned data folded with the eclipse period 0.26687 d and an arbitrary time zero-point. Right: The out-of-eclipse part of the observed light curve folded with a period of 0.213236 d.

Fig. 2 shows the standard periodogram of all out-of-eclipse flux measurements. In the left plot, the entire collection of Q14 flux measurements is used. The peak at  $P_o$  and its harmonics represent the eclipses, but they are not the largest signals in the data. In order to remove the eclipses, we discarded all data points within a window of 0.0678 d centered on each eclipse minimum. This simple technique allows us to suppress a series of signals in the periodogram caused by the eclipse of limited duration and strongly non-sinusoidal shape. The remaining peaks in Fig. 2, right, reveal the presence of other periodic signals. The height of each peak is exactly the amplitude of the best-fitting sinusoid (with a free phase) at the corresponding frequency. The most powerful out-of-eclipse sinusoidal signal has a period of 0.2132(3) (in Q14) and an amplitude of  $3.94 \text{ e}^- \text{ s}^{-1}$ . It is in fact more powerful than the eclipses. We will use  $P_e$  to denote this period. There are two less prominent peaks at 0.10663(7), 0.07107(4) d, with amplitudes 0.94,  $0.42 \text{ e}^- \text{ s}^{-1}$ , which are obviously the second and third harmonics of the main mode, i.e.,  $P_e/2$  and  $P_e/3$ . Their presence signifies a non-sinusoidal shape of the mode, which is also visible in Fig. 1, right. Finally, there seems to be a few other prominent signal with a periods  $P_a = 0.1185(1)$  (amplitude  $1.26 \text{ e}^- \text{ s}^{-1}$ ), 0.08207 d, and 0.06277 d, which are not present in the full-data periodogram on the left. We posit that it is an artifact, which is sometimes called alias in the literature. It is caused by the removal of segments of data with a period of  $P_e$  and the interference of these blank spaces with the actual periodicity. Indeed, we observe that  $1/P_a = 1/P_e + 1/P_o$  to within 0.15% of its value, and the other periods are exactly  $1/(1/P_e + k/P_o)$ ,  $k = 2, 3$ .

The presence of a periodic signal with  $P_e$  is quite striking, because the ratio of the two physical periods,  $P_o/P_e$  is equal to 5/4 within 0.16% of its measured value. This can hardly

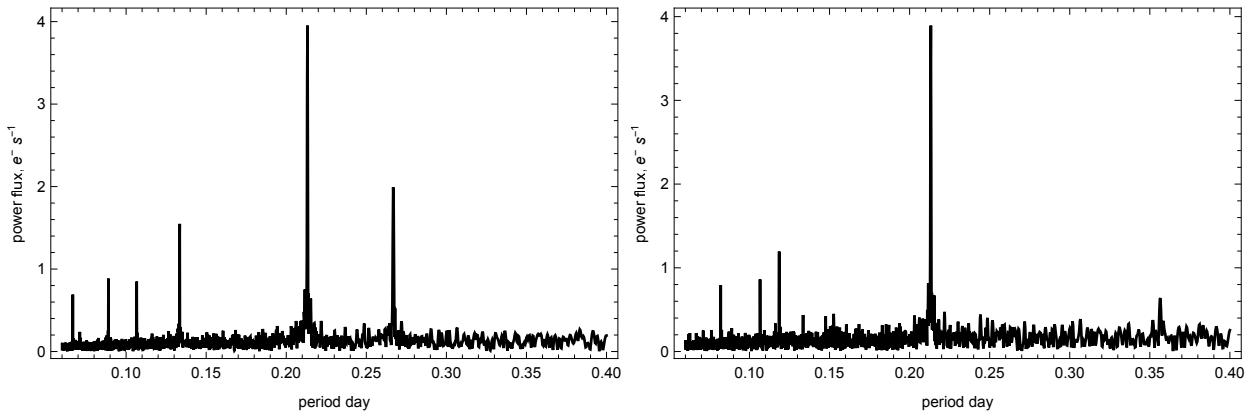


Fig. 2.— Amplitude periodograms of the long-cadence light curve of KIC 5773205 in Q14. Left: The entire light curve data are included, showing the two main periodicities and their harmonics. Right: Only the out-of-eclipse segments are included, removing the eclipse signal but introducing aliases.

be attributed to chance, hence, the signals should be interrelated. The star and the eclipsing companion are separated by roughly  $1.5 R_{\odot}$  (assuming a total mass of  $0.4 M_{\odot}$ ), which may be close enough to generate tidal deformations of the star. The ellipsoidal deformation and the related gravity-dependent surface brightness modulation emerge in light curves as a mainly semidiurnal variation, i.e., with a period of  $P_o/2$ . Contrary to this expectation, we do not find any signal of note at  $P_o/2$ , but instead find a strong quasi-sinusoidal signal at  $4 P_o/5$ .

#### 4. The origin of commensurability

As in many other cases of unclear interpretation of periodic signals observed from stars, whether photometric or spectroscopic, there are three general routes that may be interrelated, viz., non-radial pulsation, rotation, and orbital perturbation (Wilson 1994; Hatzes & Cochran 1999). Manifestations of these mechanisms are so similar in the limited data that any interpretation bears a good deal of uncertainty. These mechanisms may also work together, as in the case of a spotted star synchronously rotating with a close companion. We explore in this study the possibility that the phases and amplitudes of the observed Fourier modes can be decisive in selecting the most likely interpretation.

To estimate the relative phase of the commensurate signals, we combine the three quarters of flux measurements into one data set by converting each quarter’s flux into relative flux deviation  $\delta F = (F - F_{\text{median}})/F_{\text{median}}$  expressed in parts per thousand (ppt). This step is required because of a different photometric setup between the quarters resulting in a much different flux level. The joint three quarters of data are cleaned of the eclipse segments and then fitted with a series of Fourier functions, which are the unity and sin- and cos-harmonics of  $P_e$ , i.e.,  $2\pi(t - t_0)/(k P_e)$ , with  $k = 1, 2, 3$ . The 7 unknown coefficients are determined in a

non-weighted least-squares solution. The amplitudes of harmonics are computed as  $\sqrt{s_k^2 + c_k^2}$ , where  $s_k$  and  $c_k$  are the fitted coefficients of the sin- and cos-terms, respectively, and the phase is defined as  $\arctan(s_k/c_k)$ . This procedure allows us to improve on the knowledge of  $P_e$  using the entire collection of data, because a slight offset in this parameter results in a clearly detectable linear trend of the measured phase. The least-squares fit is generated for 29 consecutive bins of flux measurements, each spanning 6.79 d. A zero-point epoch  $t_0 = 1339.35$  (barycentric Julian day minus 2454833.0) is chosen to produce zero phases (on average) for the dominant harmonic  $\sin(2\pi(t - t_0)/P_e + \phi)$ , i.e., at this time the main Fourier term crosses zero while increasing.

The resulting phase determinations for the first harmonic ( $k = 1$ ) show a remarkably flat curve, i.e., no time dependence, and a standard deviation of  $2.5^\circ$  around the mean of  $-0.1^\circ$ . This precludes a more distant and sufficiently massive orbiting companion with periods up to  $\sim 1$  year, which would have caused a measurable light travel time (LTTE) effect. The improved period based on the three quarters of data is  $P_e = 0.213236(2)$  d. The phases of the second harmonic show no time dependence either, but are of more modest precision, grouping around  $80.8^\circ$  with a std of  $10.7^\circ$ . This value means that the term is close to its maximum value at the chosen reference epoch. The fitted Fourier harmonics and the mean flux can be subtracted from the entire light curve (including the eclipse segments), and then the data can be time-folded with the  $P_o$  period. The result for Q16 is shown in Fig. 3, left. A remarkable improvement in the scatter of data points is obvious, and the shape of the eclipse, as well as the out-of-eclipse behavior, are more visible now. The eclipse is distinctly triangular, without a flat bottom, which hints at a companion of comparable radius and a tangent, partial eclipse. Fig. 3, center, shows the out-of-eclipse part of the light curve for Q16 folded with  $P_e$  and the same reference epoch. We note that there are times, separated by  $5P_e$ , when the eclipse minimum nearly coincides with the main sinusoid minimum. At these instances, the eclipsing companion is the closest to the line of sight, and the periodic part of the flux is the dimmest. The cleaned out-of-eclipse part of the light curve folded with  $P_e$  (Fig. 3, right) is flat with a std scatter of  $1.8 e^- s^{-1}$ .

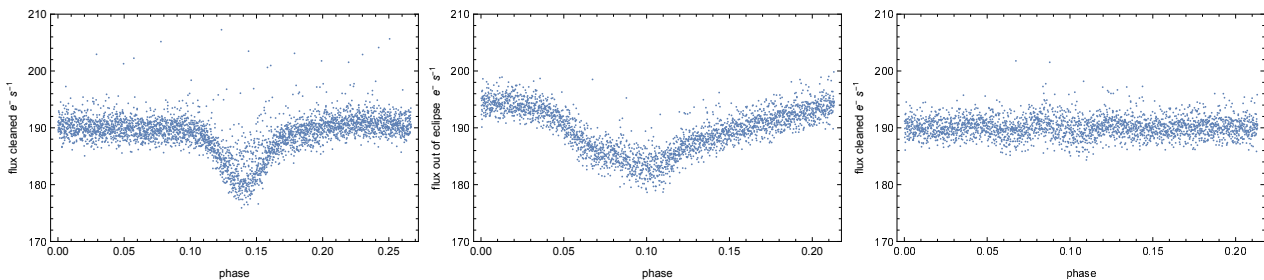


Fig. 3.— Folded light curves of KIC 5773205 in quarter 16. Left: Light curve with 6 sinusoidal harmonics of the  $P_e$  variation filtered out, folded with the orbital period  $P_o = 0.2668707$  d. Center: Out-of-eclipse segments of the light curve folded with the period  $P_e = 0.213236$  d. Right: Out-of-eclipse segments of the light curve with 6 sinusoidal harmonics of the  $P_e$  variation filtered out, folded with the period  $P_e = 0.213236$  d.

#### 4.1. Tidal deformation caused by a tertiary companion

Many eclipsing stars with periods shorter than 1 day show signs of ellipsoidal variation caused by the tidal deformation of the orbiting companions. The perturbing tidal potential may have several significant modes (depending mostly on the relative orbital separation and the eccentricity), but the greatest mode for nearly circular orbits is semidiurnal, whose frequency is exactly twice the orbital frequency. For KIC 5773205, the presence of an orbiting companion is witnessed by the periodic eclipse, but it can not be responsible for the sinusoidal variation because of the unmatched period. The only remaining possibility is a third component of the system orbiting the primary with a period of  $2 P_e$  and generating the observed ellipsoidal light curve.

This explanation meets a few crucial difficulties. The orbits of the hypothetical tertiary and the eclipsing companions should be in the 8/5 period commensurability, i.e., in a mean motion resonance (MMR). Although 8/5 MMRs have been detected for exoplanet systems (Barclay et al. 2013; Gillon et al. 2017), they seem to arise when more than two companions are present in a tightly packed configuration, and their masses are much smaller than the mass of the star. In this case, a significant stellar mass is required to produce ellipsoidal variations of the observed amplitude, which makes long-term dynamical stability of the system questionable.

The relative flux variation in each of the tidally interacting stars can be written as (Morris & Naftilan 1993):

$$F/F_0 = \bar{F} + q \sum_{n,k} \alpha_{nk} \left(\frac{R}{a}\right)^n f_{nk}(i) \cos k\phi \quad (1)$$

where  $F_0$  is the flux from a non-perturbed star,  $\bar{F}$  is the mean disk-integrated, relative flux from a perturbed star,  $\alpha_{nk}$  are coefficients, which depend on the limb-darkening and gravity-darkening parameters,  $f_{nk}$  are functions of  $i$ , which is the inclination of the orbital axis to the line of sight, and  $\phi$  is the perturber’s longitude with respect to the line of sight (zero at the eclipse minimum). For detached systems,  $R/a$  is small, and only a limited number of terms may be of interest. The coefficients and inclination functions of all significant terms are listed in Table 1.  $R$  is the radius of the perturbed star, and  $q$  is the ratio of the perturber’s mass and the mass of the perturbed star. The lowest power of  $R/a$  in the 32 semidiurnal term marks it as by far the largest. For KIC 5773205, the observed amplitude of the main harmonic is approximately 30 ppt, and the estimated  $R/a$  is greater than 3 (but can be as large as 6). The mass of the tertiary companion then would be comparable to, or several times greater than the mass of the eclipsed M dwarf, which seems improbable.

Perhaps, a more specific test comes from the consideration of estimated amplitudes and phases of the periodic signal. Table 1 suggests that the semidiurnal harmonic should be much greater than the other terms, if detectable at all. Interpreting the strongest periodicity as the 32 term (proportional to  $\cos 2\phi$ ), we also find a clearly present  $P_e/2$  harmonic, which would be the 54 term, but no sign of the 41 or 43 terms. The former can vanish if the inclination

is close to  $63.43^\circ$  due to its inclination function, but the latter should always be larger in amplitude than the 54 term. However, we note that Eq. 1 and Table 1 are derived for a circular orbit. Deformations caused by an eccentric perturber can have a different distribution of power between the harmonics with the peak shifted toward higher orders of the perturbing potential. But this implies an exotic triple system with a stellar-mass outer companion in a rather eccentric orbit, in which the eclipses are caused by a smaller mass inner companion, such as a bloated giant planet.

Finally, the signs of  $\alpha_{32}$  and  $\alpha_{54}$  are opposite (Table 1). This means that the maxima of these two harmonics should coincide when  $\phi = \pi/2$ , but the minima cannot coincide. On the contrary, the observed phases of these two terms suggest that their minima almost overlap at times separated by  $P_e$ , which is characteristic of eclipses but not of ellipsoidal variation.

## 4.2. Yin-yang stars

M dwarfs display a wide range of rotation periods, which are correlated with their age and activity level. The majority of old, inactive stars rotate slowly, with insignificant consequences for the light curve. The system of KIC 5773205 is moderately active, as witnessed by the frequent flares, which is expected of a close binary. It can not be precluded that one of the components rotates fast and modulates a light curve with the observed period  $P_e$ . Stars like the Sun have surface brightness irregularities, such as spots and plages, that are small-scale and short-lived. The observed photometric effects are stochastic and low-amplitude (Makarov et al. 2009), making their detection a difficult task. On the other hand, active dwarfs in binary systems may have large surface structures occupying a significant fraction of the visible disk. Presumably, they are also long-lived and appear in the line of sight for many consecutive rotation periods, generating a strong modulation signal.

The amplitude of a single spot modulation in relative flux is proportional to  $(1 - f_s)r_s^2$ , where  $f_s$  is the contrast of the spot (close to unity) and  $r_s$  is the central angle spanned by the spot's radius in radians. The deficit (or excess) of flux in the spot,  $1 - f_s$  is a small positive or negative number, which is not expected to exceed several percent in absolute value. A rough estimation reveals that in order to generate a 3% modulation observed for KIC 5773205, the radius of the spot structure should approach  $\pi/2$ , i.e., the structure should fill almost half of the surface. In this extreme scenario, the star is painted different colors on two sides. Like with the ellipsoidal variation scenario, the first crucial problem is that the observed sinusoidal variation is too large.

The main mode of a surface structure modulation is close to the equatorial rotation period within the spread caused by the differential rotation and the latitude. The nearly perfect 5/4 commensurability between  $P_o$  and  $P_e$  implies that the star rotates by exactly 25% faster than the occulter's orbital motion. This condition is called spin-orbit resonance, and it is a natural consequence of the frequency-dependent secular tidal torque for solid planets (e.g.,

Efroimsky 2012; Efroimsky & Makarov 2013). Stars, however, are closer to the “semiliquid” regime where the main viscous response to tidal perturbation is greatly smoother in frequency, and the absence of a permanent shape results in the pseudosynchronous stable equilibrium (Murray & Dermott 1999; Makarov 2015). In that state, the perturbed body rotates faster than the synchronous rate, and the offset in frequency is a smooth function of the orbital eccentricity. There is no condition that forces the equilibrium rate to be in exact integer ratio to the mean motion.

On the remote chance that the star has an unexpectedly high viscosity and a finite rigidity (caused by magnetic turbulence, for example), we can consider well understood planetary resonances. The tidal modes in this case split into a spectrum defined by 4 integer indices  $lmpq$ :

$$\omega_{lmpq} = (l - 2p + q)n - m\Omega, \quad (2)$$

where  $n = 2\pi/P_e$  is the mean motion,  $\Omega$  is the spin rate,  $l = 2, 3, \dots$ ,  $p = 0, \dots, l$ ,  $m = 0, \dots, l$ , and  $q$  is any integer between  $-\infty$  and  $+\infty$ . A spin-orbit resonance occurs when  $\omega_{lmpq} = 0$ .  $m$  is the number of sectorial spherical harmonics in the perturbation potential, which is limited to the degree  $l$ . The lowest degree of a  $\Omega/n = 5/4$  spin-orbit resonance is then  $l = 4$ . However, the degree-4 tidal perturbation should be vanishingly small compared with the main  $l = 2$  (quadrupole) perturbation for well detached systems, because the potential is proportional to  $(R/a)^{l+1}$  (e.g, Kumar et al. 1995; Pfahl et al. 2008) for a given tidal mode. We conclude that photospheric structures and a tidal spin-orbit resonance can hardly explain the detected photometric signals.

### 4.3. Heartbeat stars

Non-radial pulsations can be perpetually excited by close companions in eccentric orbits and show up as quasi-sinusoidal variations at frequencies in integer-number commensurabilities with the orbital frequency. KOI-54 is perhaps the most impressive example of the class with sharp brightening peaks in the light curve separated by an orbital period of 41.8 d and tidally excited non-radial pulsations with frequencies that are exact 90th and 91st integer multiples of the orbital frequency (Welsh et al. 2011). The class of eccentric heartbeat binaries is characterized by orbital periods of 4–20 d and often pulsations at higher frequencies (Thompson et al. 2012). As with KOI-54, the pulsation frequencies are large multiple integers of the tidal frequency. They show up in the time-folded light curves as wiggles overlaying the eclipsing and, sometimes, ellipsoidal variations. HD 183648 is an interesting example of a low-eccentricity heartbeat binary with an out-of-eclipse semidiurnal periodicity, which seems to have the opposite phase to the expected ellipsoidal modulation (Borkovits et al. 2014). One may wonder if the out-of-eclipse modulation for HD 183648 is also a heartbeat pulsation in a 2:1 resonance with the orbital period, and its observed phase is simply caused by the periastron direction being at roughly the right angle from the line of sight. Other cases of detected period commensurability include the 6/1 ratio in the HAT-P-11 planetary system (Béky et al. 2014), which

is interpreted as a spin-orbit resonance and a persistent surface spot, and a 5/3 ratio for the KOI-13 system (Szabó et al. 2012), also interpreted as a spin-orbit resonance. We discussed in the previous paragraphs why this interpretation is unlikely.

Rodríguez-López et al. (2012) suggested possible mechanisms of pulsation for M dwarfs and conditions of their detection. One of the mechanisms is expected to produce pulsations in the period range of interest, i.e., a few to several hours depending on the mass, but it is caused by the strong temperature dependence of deuterium burning, and therefore, applies only to very young stars. Fully convective old stars of low mass can pulsate due to He<sup>3</sup> burning, but the period is expected to be shorter than 41 min. Attempts to detect these pulsations have been unsuccessful (Rodríguez-López et al. 2015; Rodríguez et al. 2016).

## 5. Summary

Gaidos et al. (2016) estimated for KIC 5773205 a radius of  $0.18R_{\odot}$  and a mass of  $0.18M_{\odot}$  with a large uncertainty. In the light of Gaia DR2 data, the star is much more distant and more luminous, with a mass of  $\sim 0.4M_{\odot}$ . Armstrong et al. (2014) estimated close effective temperatures of the two companions in the range 3500–3600 K, but a radius ratio of  $0.5 \pm 0.4$ . The paucity of accurate data leaves room to speculation about the nature of this binary. The eccentricity of the system can be significant, based on the absence of secondary eclipses, but perhaps not very high, because no periastron brightening is present either. We considered three possible scenarios for the discovered photometric commensurable periodicities and found two of them to be rather outlandish. An ellipsoidal tidal deformation does not pass because it requires a stellar-mass tertiary component in a 8/5 MMR, and the amplitudes and phases of the harmonics do not match the expectation. A persistent photospheric spot would have to be very large or exceptionally dark to explain the observed amplitude of the main mode, and the rate of rotation would need to be in a nearly perfect 4/5 spin-orbit resonance, for which we do not see a theoretical justification.

This leaves us with the possibility of a non-radial pulsation excited by tidal interaction.

Table 1: Theoretical coefficients and inclination functions of ellipsoidal flux variations for the  $V$  and  $R$  photometric bands and a circularized orbit.

		$f(i)$	$V$	$R$
$\alpha_{32}$		$\sin^2 i$	−1.21	−1.14
$\alpha_{41}$	$4 \sin i - 5 \sin^3 i$		+0.12	+0.09
$\alpha_{43}$		$\sin^3 i$	−0.21	−0.15
$\alpha_{52}$	$6 \sin^2 i - 7 \sin^4 i$		−0.21	−0.22
$\alpha_{54}$		$\sin^4 i$	+0.37	+0.39

The model by Kumar et al. (1995) of the class now known as heartbeat stars predicts a large morphological variety of signals driven by the multitude of geometrical and orbital configurations. This model has often (but not always) been successful in describing the periastron impulse-like variations in Kepler light curves (Thompson et al. 2012). In KIC 5773205, we may be seeing a new type of heartbeat stars without prominent periastron impulses but with pulsations that are tightly spaced from the excitation frequency. It is possible that the damping time is short for the proposed mechanisms and they become prominent only when excited by a variable tidal force in sufficiently close binaries. Such binaries are usually active and flaring, further concealing the intrinsic pulsation. Interestingly, we find an additional strong periodicity at the high-frequency end of the available spectrum with a period of 0.022597 d = 32.54 min and an amplitude of  $3.2 \text{ e}^- \text{ s}^{-1}$ , but it cannot be validated being too close to the long cadence observation frequency. But the 5.1-hr signal we discovered does not currently have a theoretical background as an intrinsic non-radial pulsation.

### Acknowledgments

This paper includes data collected by the Kepler mission. Funding for the Kepler mission is provided by the NASA Science Mission directorate. Some of the data presented in this paper were obtained from the Mikulski Archive for Space Telescopes (MAST). STScI is operated by the Association of Universities for Research in Astronomy, Inc., under NASA contract NAS5-26555. Support for MAST for non-HST data is provided by the NASA Office of Space Science via grant NNX09AF08G and by other grants and contracts. This research has made use of the VizieR catalogue access tool, CDS, Strasbourg, France. The original description of the VizieR service was published in A&AS 143, 23.

### REFERENCES

- Armstrong, D.J., Gómez Maqueo Chew, Y., Faedi, F., Polacco, D. 2014, MNRAS, 437, 3473
- Barclay, T., Rowe, J.F., Lissauer, J.J., et al. 2013, Nature, 494, 452
- Béky, B., Holman, M.J., Kipping, D.M., Noyes, R.W. 2014, ApJ, 788, 1
- Borkovits, T., Derekas, A., Fuller, J., et al. 2014, MNRAS, 443, 3068
- Brown, A. G. A., Vallenari, A., Prusti, T., and Gaia Collaboration, 2018, A&A, 616, A1
- Christiansen, J.L., Jenkins, J.M., Caldwell, D.A., et al. 2012, PASP, 124, 1279
- Conroy, K.E., Prša, A., Stassun, K.J., et al. 2014, AJ, 147, 45
- Chambers, K.C., Magnier, E.A., Metcalfe, N., et al. 2016, arXiv:1612.05560

- Efroimsky, M. 2012, ApJ, 746, 150
- Efroimsky, M., Makarov, V.V. 2013, ApJ, 764, 26
- Gaidos, E., Mann, A.W., Kraus, A.L., Ireland, M. 2016, MNRAS, 457, 2877
- Gillon, M., Triaud, A.H.M.J., Demory, B.-O., et al. 2017, Nature, 542, 456
- Hatzes, A.P., Cochran, W.D. 1999, MNRAS, 304, 109
- Henry, T.J., Jao, W.C., Subasavage, J.P., et al. 2006, AJ, 132, 2360
- Kirk, B., Conroy, K., Prša, A., et al. 2016, AJ, 151, 68
- Kumar, P., Ao, C.O., Quataert, E.J. 1995, ApJ, 449, 294
- Lurie, J.C., Vyhmeister, K., Hawley, S.L., et al. 2017, AJ, 154, 250
- Makarov, V.V., Beichman, C.A., Catanzarite, J.H., et al. 2009, ApJ, 707, L73
- Makarov, V.V. 2015, ApJ, 810, 12
- Makarov, V.V., Goldin, A. 2016, ApJS, 224, 19
- Makarov, V.V., Goldin, A. 2016, ApJ, 833, 78
- Makarov, V.V., Goldin, A. 2017, ApJ, 845, 149
- Morris, S.L., Naftilan, S.A. 1993, ApJ, 419, 344
- Murray, C.D., Dermott, S.F. 1999. *Solar System Dynamics*. Cambridge University Press, Cambridge UK
- Parsons, S.G., Agurto-Gangas, C., Gansicke, B.T., et al. 2015, MNRAS, 449, 2194
- Pfahl, E., Arras, P., Paxton, B. 2008, ApJ, 679, 783
- Ritter, H., Kolb, U.. 2003, A&A, 404, 301
- Rodríguez-López, C., MacDonald, J., Moya, A. 2012, MNRAS, 419, L44
- Rodríguez-López, C., Gizis, J.E., MacDonald, J. 2015, MNRAS, 446, 2613
- Rodríguez, E., Rodríguez-López, C., López-González, M.J., et al. 2016, MNRAS, 457, 1851
- Slawson, R.W., Prša, A., Welsh, W.F., et al. 2011, AJ, 142, 160
- Szabó, G.M., Pál, A., Derekas, A. 2012, MNRAS, 421, L122
- Thompson, S.E., Everett, M., Mullally, F. et al. 2012, ApJ, 753, 86

Welsh, W.F, Orosz, J.A., Aerts, C., et al. 2011, ApJS, 197, 4

Wilson, R.E. 1994, PASP, 106, 921

